EPJ Web of Conferences **308**, 01010 (2024) https://doi.org/10.1051/epjconf/202430801010
ISRD 17

Perovskite-based detector for reactor dosimetry monitoring

Pavao Andricevic[1,2,*], *Pavel* Frajtag[3], *Peter* Szirmai[2], *Gábor* Náfrádi[4], *Márton* Kollár[2], *László* Forró[2,5], *Endre* Horváth[2], and *Andreas* Pautz[3]

[1]Department of Physics, Technical University of Denmark, Risø campus, 4000 Roskilde, Denmark
[2]Laboratory of Physics of Complex Matter, Ecole Polytechnique Fédérale de Lausanne, 1015 Lausanne, Switzerland
[3]Laboratory of Reactor Physics and System Behaviour, Ecole Polytechnique Fédérale de Lausanne, 1015 Lausanne, Switzerland
[4]ISIS Pulsed Neutron and Muon Source, STFC Rutherford Appleton Laboratory, Harwell Oxford, Didcot, OX11 0QX UK
[5]University of Notre Dame, 204A Nieuwland Science Hall, Notre Dame, IN 46556, USA

Abstract. Hybrid halide perovskites have demonstrated significant efficiency in detecting a broad spectrum of high-energy radiation, including X-rays, gamma rays (γ-rays), and neutrons. Given the common occurrence of mixed radiation fields, we investigated the performance of a perovskite-based detector in a neutron-gamma mixed field. A large methylammonium lead tribromide ($MAPbBr_3$) single crystal (SC) was synthesized via the oriented crystal-crystal intergrowth method. This SC was used to fabricate a gamma detector with carbon electrodes, which was tested in the CROCUS zero-power reactor cavity. The detector's photocurrent response exhibited a strong correlation with known gamma dose rates, as measured by an ambient Berthold LB 112 gamma probe, facilitating the accurate conversion of photocurrent to dose rate. Notably, the device did not exhibit degradation under neutron radiation exposure. To further assess the impact of neutrons, X-ray diffraction and electron paramagnetic resonance analyses were performed on small $MAPbBr_3$ SCs grown by inverse temperature crystallization. These SCs were irradiated within the CROCUS reactor core and by a Pu-Be neutron source at liquid nitrogen temperature. Our findings indicate that the perovskite material can withstand the nominal in-core operation conditions of the CROCUS reactor. Additionally, it endures irradiation at liquid nitrogen temperature, corresponding to a fast neutron fluence of approximately 10^{10} cm^{-2} and a gamma radiation dose of about 50 Gy, confirming only the temporary creation of defects. No signs of long-term deterioration were observed, suggesting a potential self-healing mechanism. This resilience positions perovskite SCs as viable candidates for in-core radiation detection, supporting the further development of miniaturized $MAPbBr_3$ SC devices for such applications.

* Corresponding author: pavaoand@gmail.com

1 Introduction

Hybrid halide perovskites (ABX_3) meet all the essential criteria for high-energy radiation detection.[1], [2] The inclusion of high atomic number (Z) elements like lead (Pb), iodine (I), and bromine (Br), coupled with the relatively high density of perovskites (4.0 g/cm³), ensures significant attenuation of high-energy photons. These materials possess large intrinsic bandgaps, which mitigate thermal noise and exhibit high resistance, thereby suppressing dark current and device noise. Additionally, they have a favorable mobility-lifetime product, facilitating efficient charge collection.[3]

Unlike market-leading crystals such as zinc-alloyed cadmium telluride (CdTe),[4] perovskite single crystals (SCs) can be synthesized from abundant and low-cost raw materials in near-room-temperature solutions without the need for expensive infrastructure.[2] Consequently, perovskite materials are promising candidates for the development of next-generation high-energy radiation detectors.

Perovskites have been extensively studied as X-ray and gamma-ray detectors. For X-rays, ultrahigh sensitivities of 2.2×10^8 μC $Gy_{air}^{-1}.cm^{-2}$ have been achieved,[5] along with low detectable dose-rate limits of just 36 $nGy_{air}.s^{-1}$.[6] Their application in production has been adopted by leading industry players such as Samsung for medical imaging.[7] Promising results have also been obtained in gamma photon detection, demonstrating high energy resolution across a wide range of gamma energies:[3], [8]–[11] from 59.5 keV (^{241}Am gamma-ray), 122 and 136 keV (^{57}Co gamma-ray), 511 keV (^{22}Na gamma-ray) to 662 keV (^{137}Cs gamma-ray), with the best spectral resolution documented at 3.8%, comparable to state-of-the-art gamma detectors.[12] Furthermore, we have previously demonstrated the capability to measure dose rates of even higher energy photons (1.173 and 1.332 MeV ^{60}Co gamma-rays) with high sensitivities by increasing the detector's active thickness to over 10 centimeters.

To date, most studies on perovskite-based radiation detection have been limited to detecting a single type of radiation within a narrow energy range.[13] In this study, we present the use of perovskite detectors in a mixed neutron-gamma field. The perovskite-based radiation detectors demonstrated the ability to monitor ambient dose rates without any performance degradation or crystal deterioration while being tested in the cavity of the CROCUS reactor and its core under few watts up to maximum nominal operation conditions corresponding to a thermal power of 100 watts. These detectors were tested in the reactor core of an experimental zero-power reactor at thermal and fast neutron fluxes on the order of 10^9 $cm^{-2}.s^{-1}$ and 10^8 $cm^{-2}.s^{-1}$, respectively, and gamma radiation dose rates in the $Sv.h^{-1}$ range, showing no decrease in operational performance. An investigation into the potential degradation of methylammonium lead tribromide SCs was conducted by irradiating identical samples under three different conditions: within the CROCUS reactor core, near a high-activity ^{60}Co source at room temperature, and with a Pu-Be source at liquid nitrogen temperature. Only when irradiated by a Pu-Be neutron source at liquid nitrogen temperature, i.e., exposed to a fast neutron fluence of approximately 10^{10} cm^{-2} and an accumulated gamma radiation dose of about 50 Gy, did the crystals exhibited temporary creation of defects, with no long-term changes in their structure observed at room temperature. This is likely due to their unique self-healing mechanism. However, it is crucial to address other factors such as high humidity, which can be detrimental to perovskites, and ensure that they are minimized or eliminated.

2 Results

Methylammonium lead tribromide ($MAPbBr_3$) was selected as the hybrid halide perovskite for detector fabrication due to its superior stability compared to its iodide

counterpart, which is more commonly used in the photovoltaic industry. A crucial factor in this choice was its capability to grow into decimeter-sized crystals (Fig. 1a). Recently, the OC2G technique was developed,[2] enabling the production of solution grown $MAPbBr_3$ crystals with a volume exceeding 1,000 cm^3 and a mass of 3 kg. In this study, a smaller crystal with dimensions of (5 x 5 x 5) cm^3, grown using this technique, was utilized for investigation.

The single crystal (SC) was coated with graphite spray on two sides, leaving a small gap in between, as depicted in Fig. 1b. Two copper wires embedded in carbon epoxy contact pads on each facet of the crystal served as biasing electrodes. It is important to note that this electrode design does not fully exploit the crystal's volume.[2] Some photocarriers cannot be harvested by the electrodes due to recombination and trapping within the SC. Implementing a volumetric electrode design with a 3D electrode pattern[14] could further enhance the device's sensitivity.

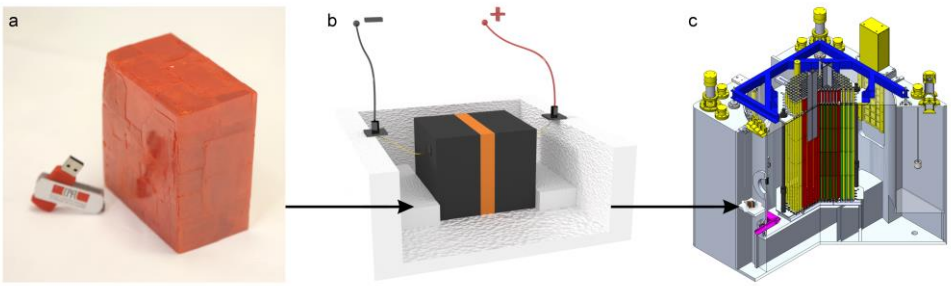

Fig. 1. (a) Solution-grown $MAPbBr_3$ crystal, (b) fabricated perovskite-based device, (c) CROCUS reactor and detector position.

The fabricated perovskite device was tested in the concrete cavity of the experimental zero-power reactor "CROCUS" at the École Polytechnique Fédérale de Lausanne (EPFL). The reactor has a maximum thermal power of 100 W, corresponding to a neutron flux of approximately 2.5×10^9 $cm^{-2}.s^{-1}$ at the core center. A schematic of the reactor setup is shown in Fig. 1c. The detector was positioned inside the concrete cavity of the reactor, outside the aluminum vessel filled with demineralized water, which contains 336 UO_2 and 176 Umet fuel rods in the inner and outer core, respectively. The experimental setup is visualized in Fig. 1c.

The perovskite detector was exposed to hard gamma rays and leaked neutrons from the reactor core. Coaxial cables connected the detector to a Keithley 2400 source meter, which measured the current generated by the perovskite detector upon radiation exposure. One advantage of the perovskite-based detector is its capability to directly measure the current generated during radiation exposure under an applied bias voltage of 1 V. A proportional relationship was observed between the measured current, gamma dose rates, and various power levels of the CROCUS reactor. This was determined through measurements taken from the neutron detector (CFUL fission chamber) positioned at the periphery of the reactor core and from the calibrated gamma probe (Berthold LB 6500-3-H10) installed in the reactor cavity. This allowed for the evaluation of dose rate and power level changes based on a simple current measurement form the perovskite-based detector.

The calibration of dose-rate measurements and the stability test of the detector at the specific position within the reactor cavity were performed through comparative measurements using the calibrated Berthold gamma probe placed adjacent to the perovskite detector. This method ensured accurate and reliable calibration of the perovskite detector´s response to radiation.

2.1 Detector response to radiation in the reactor cavity

As illustrated in Fig. 2, there is a strong correlation between the measured signals: red for photocurrent, blue for neutron detector count rate, and green for gamma dose-rate. During the initial measurement sequence, the reactor power was increased from 1 to 20 W (Fig. 2a). The perovskite photocurrent exhibited an overshoot relative to the mean value with each increment in reactor power, followed by a gradual decrease over time. This behavior may indicate perovskite degradation or an increase in environmental humidity. [15], [16] Alternatively, it could be attributed to the total "dark" or "baseline" current, which slightly increases over time and is subtracted from the measured photocurrent.

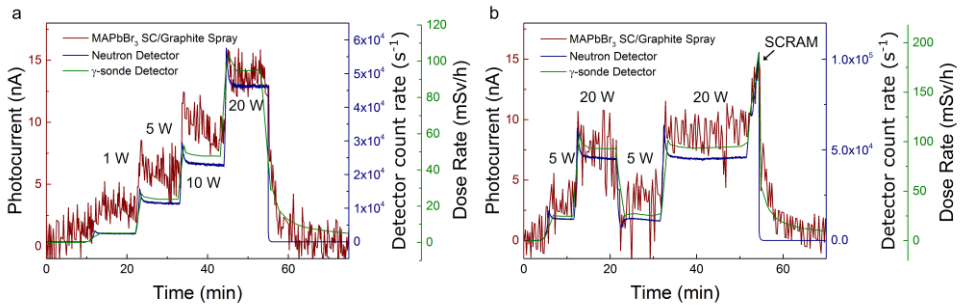

Fig. 2. Photocurrent measured from the perovskite-based detector compared to neutron detector count rate and gamma dose-rate measurements in the reactor and its cavity, respectively.

A second measurement sequence involved varying the reactor power from 5 to 20 W, followed by a reduction to 5 W, and a subsequent increase back to 20 W (Fig. 2b). Different time intervals were used for measurements at set power levels. In this instance, a more stable baseline current was achieved prior to the start of the measurements, leading to a more consistent generated photocurrent. The photocurrent signal closely tracked the dose-rate measurement of the gamma sensor. The detector functioned under operational conditions without exhibiting any performance degradation, even at a dose rate of 100 $mSv.h^{-1}$ corresponding to 20 W for approximately 20 minutes. Over the course of the one-hour measurement, the detector accumulated a gamma absorbed dose of approximately 40 mGy. Notably, the neutron fluence at the measurement position outside the reactor vessel in the reactor cavity reached an order of 10^9 cm^{-2}.

Finally, the reactor power was further increased, reaching gamma dose-rates of nearly 200 $mSv.h^{-1}$, before performing a rapid emergency shutdown (SCRAM) to test the detector's response time. Within less than 0.5 seconds after the reactor shutdown, the photocurrent signal decreased by more than 50% and continued to decline slowly, mirroring the gamma sensor dose rate.

2.2 Perovskite-based detector degradation

After conducting additional measurement sequences, the detector's performance remained unaffected by radiation within the reactor cavity. This suggests that perovskite-based detectors, which can be fabricated in various shapes and dimensions, have the potential for use in reactor in-core dosimetry. In such applications, the single crystal is expected to withstand even higher gamma dose rates and neutron fluences. Therefore, for a perovskite-based device to operate effectively in the CROCUS reactor core, it must endure gamma dose rates on the order of 10^4 $mSv.h^{-1}$ and neutron fluxes exceeding 10^9 $cm^{-2}.s^{-1}$.

To evaluate potential degradation of $MAPbBr_3$ perovskite, small identical single-crystal (SC) samples measuring (1.0 x 1.0 x 0.5) cm^3, grown using the inverse temperature crystallization method,[2] were placed in a tube and inserted into an empty control rod channel in the CROCUS reactor core, as depicted in Fig. 3a. It should be noted that the CROCUS reactor can be operated by varying the water level in the reactor vessel or by using two B_4C control rods, which may not be present in certain core configurations as shown in Fig. 3a. The reactor was operated for two hours at a power level of 20 W and a primary water temperature of (20.1 ± 0.2) °C, generating an in-core thermal neutron flux of approximately 5×10^8 $cm^{-2}.s^{-1}$ alongside with significant background gamma radiation. We estimate that the cumulative thermal and fast neutron fluences experienced by the perovskite sample at the irradiation position were on the order 10^{12} cm^{-2} and 10^{11} cm^{-2}, respectively, with a corresponding gamma absorbed dose of about 3.8 Gy. Simultaneously, another $MAPbBr_3$ SC sample was positioned in front of a 269 GBq ^{60}Co source, emitting 1.17 and 1.33 MeV gamma-rays at an equivalent dose rate of 2.3 $Sv.h^{-1}$. This dose rate was deduced from the measurements using a calibrated gamma probe (Berthold LB-6500-3-H10), placed at a distance ensuring the dose rate limit (≤ 1 $Sv.h^{-1}$) specified by the manufacturer (Fig. 3b). This sample was irradiated for the same two-hour duration, accumulating a gamma absorbed dose of about 4.6 Gy.

Subsequently, X-ray diffraction (XRD) measurements were conducted on both SC samples using a commercial PANalytical Empyrean diffractometer. The XRD data presented in Fig. 3c compare the signals from both irradiated samples with the XRD signal from an unirradiated sample. Characteristic $MAPbBr_3$ peaks were identifiable in all XRD measurements, with no indications of a degraded phase such as lead bromide ($PbBr_2$).[17], [18]

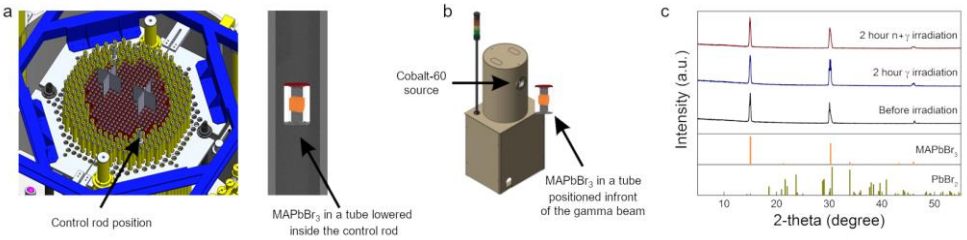

Fig. 3. Schematic of the SC locations irradiated (a) in the CROCUS reactor core and (b) by gamma-rays from a ^{60}Co source, (c) XRD measurements of the SC before and after the irradiations, compared to typical peaks of $MAPbBr_3$ and $PbBr_2$.

An electron paramagnetic resonance (EPR) technique was employed to further investigate potential defects within the perovskite bulk material. Measurements were conducted using a Bruker ELEXSYS X-band spectrometer. EPR is a highly sensitive and contactless method for detecting and quantifying paramagnetic defect concentrations down to parts per million (ppm) levels in bulk materials.[19] Due to its high sensitivity, EPR has become an indispensable tool for investigating defect states.

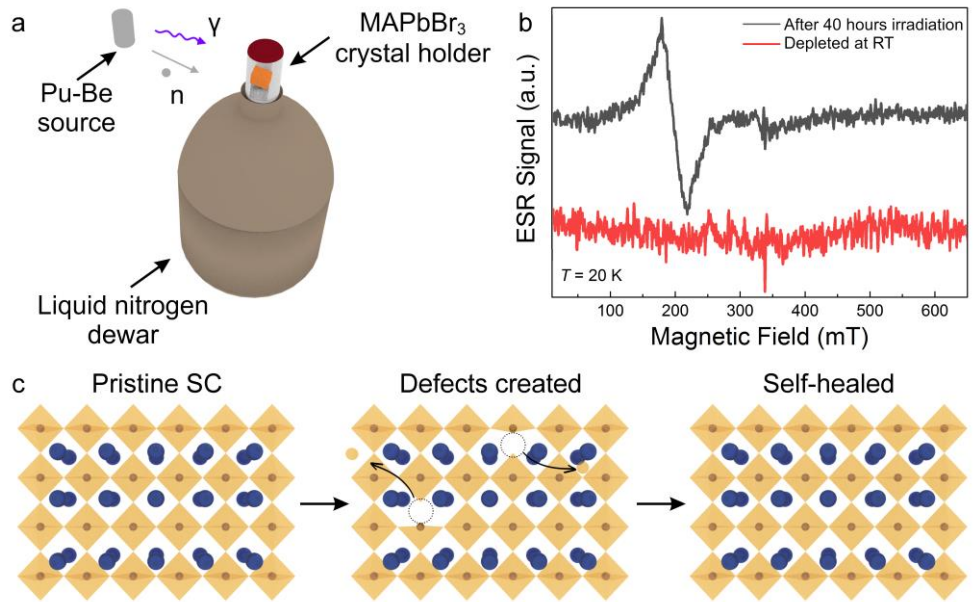

Fig. 4. (a) Schematic of a $MAPbBr_3$ SC irradiated by a Pu-Be source, (b) ESR measurements of the SC after 40 hours of irradiation, (c) Schematic representation of the self-healing behaviour of perovskite.

However, direct EPR measurements in halide perovskite structures are often limited because many defect states are EPR-silent.[20] Despite this limitation, an early study on MAPbI3 demonstrated the formation of various radical species upon exposure to intense low-temperature UV and electron irradiation, which were successfully identified using EPR.[21]

A similar approach was applied in this study to investigate the effects of gamma and neutron irradiation. A small $MAPbBr_3$ SC was exposed to radiation from a plutonium-beryllium (Pu-Be) source for 40 hours at liquid nitrogen temperature (77 K) (Fig. 4a). The Pu-Be source, with an activity of 185 GBq, produced an estimated fast neutron fluence of approximately 10^{10} cm^{-2} and a gamma radiation absorbed dose of about 50 Gy at the sample position. The selection of a Pu-Be source over the CROCUS reactor for this study was based on practical considerations, allowing for low-temperature irradiation prior to the EPR measurements. An EPR signal was observed at several temperatures below 77 K, and its Curie-like paramagnetic temperature dependence was confirmed ($\chi \propto 1/T$). After the low-temperature measurements, the sample was warmed to room temperature. As shown in Fig. 4b, room-temperature heat treatment led to the disappearance of the EPR signal. The EPR signal's g-factor was close to g=4, corresponding to triplet defect states. The disappearance of the EPR signal suggests a possible depletion of these defect states. Therefore, it can be concluded that gamma and neutron irradiation do not create spin-bearing defects in the perovskite SC, and these defects can only be trapped in existing triplet states.

This observation implies that any damage created in the perovskite SC after exposure to radiation will return to its initial condition at room temperature, exhibiting the perovskite's self-healing behavior.[2], [22], [23] Hybrid halide perovskites possess a soft crystal structure, allowing halide ions to migrate easily within the large ionic crystal lattice.[24]–[27] Consequently, it is hypothesized that if an ion is displaced from its equilibrium position, forming a point defect such as a vacancy, it can migrate back to the same position and chemically interact to restore the initial condition, as depicted in Fig. 4c.

This self-healing property is well-documented in perovskite-based devices, particularly in solar cells.[28]–[30]

2.3 In-core reactor detection

Perovskite-based detectors have demonstrated resilience against neutron and gamma radiation, exhibiting no significant long-term degradation. The subsequent objective was to assess the feasibility of utilizing a $MAPbBr_3$ SC device as an in-core detector for the CROCUS reactor. While a robust gamma radiation response from perovskite-based detectors is anticipated, the neutron detection capabilities of such devices within a reactor core remain uninvestigated.

Recent observations have revealed that incorporating a gadolinium (Gd) foil in front of the $MAPbBr_3$ SC device enables efficient detection of thermal neutron flux.[31] Neutrons absorbed by the Gd foil are converted into γ-rays,[32] which subsequently generate photo-induced charge carriers within the SC. These photo-carriers contribute to the electric current, thereby providing quantitative information regarding the intensity of thermal neutrons. Based on these findings, we have synthesized a MAPbBr3 SC encapsulating a Gd_2O_3 pellet disc, as illustrated in Fig. 5a.[31] This integrated oxide converter layer simplifies the detector architecture and enhances detection efficiency by maximizing the useful solid angle to 4π steradians.

However, such a device is incapable of differentiating between contributions from neutrons and ambient gamma rays within a nuclear reactor environment. To address this limitation, a reference perovskite gamma detector devoid of the Gd_2O_3 neutron converter was fabricated and employed for comparative measurements.

Two $MAPbBr_3$ SC devices of identical dimensions, one incorporating a Gd_2O_3 neutron converter layer and the other without, were mounted onto a coaxial cable. Electrical connections were established using gold wires attached to the perovskite SCs with carbon paste, as depicted in Fig. 5a. These compact perovskite devices were specifically designed to fit within an empty control rod channel (inner diameter 17.3 mm) in the CROCUS reactor core, as shown in Fig. 3a. Due to constraints in the experimental setup, simultaneous testing of the two devices was not feasible; thus, they were tested sequentially. For both measurements, two "on-off" sequences were executed, wherein the reactor power alternated between 0 and 1 W every 10 minutes. At the conclusion of these measurements, the power was abruptly increased, resulting in an off-scale peak, and a voluntary SCRAM by a reactor power limit was initiated to evaluate the detectors' response times. Due to the off-scale nature of the peak, the entire peak is not displayed in the data presented in Fig. 5b. Displaying the full peak would compromise the resolution and comparison of the measured data prior to the SCRAM. The comparison of detector signals is illustrated in Fig. 5b. The average photocurrents of the devices with and without the Gd_2O_3 disc at 1 W were determined to be (0.60 ± 0.08) nA and (0.10 ± 0.02) nA, respectively. The observed photocurrent difference of 0.5 nA corresponds to the neutron intensity within the reactor core.

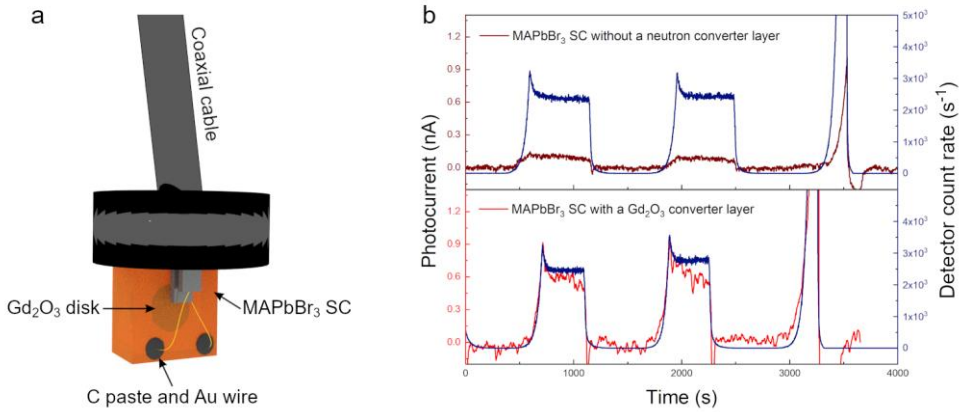

Fig. 5. (a) Perovskite-based detector fabricated from a $MAPbBr_3$ SC grown around a Gd_2O_3 pellet disc, (b) Comparison of signals from $MAPbBr_3$ SC detectors with and without a Gd_2O_3 neutron converter layer to the CFUL neutron detector count rate.

Measurements were conducted at the reactor power level of 1 W due to an initial observation of significant baseline current drift at power levels exceeding 1 W. The photocurrent responses of both detectors correlated satisfactorily with the power increase, as illustrated in Fig. 5. However, there was a noticeable decrease in photocurrent when the reactor power level was maintained steady at 1 W. X-ray diffraction (XRD) measurements at room temperature of the perovskite crystals, conducted before and after irradiation, did not reveal any phase degradation. Furthermore, both detectors remained functional without any changes before and after irradiation in the reactor core. Therefore, the observed photocurrent drift may be attributed to device degradation during operation, followed by a self-healing mechanism.

A second potential cause for the observed photocurrent drift could be the high humidity levels in the control rod channel and reactor cavity during operation. Humidity levels in the reactor cavity can exceed 80% during operation. High humidity has been shown to have a detrimental effect on all perovskite materials, including $MAPbBr_3$, which is known to be the most stable compound in this material family.[26], [33] Similar photocurrent instabilities have been previously reported for perovskite-based devices operating in high humidity environments. Fig. 6 illustrates measurements taken in the CROCUS reactor using a poorly isolated perovskite-based detector ramped from 0 to a maximum power of 100 W, where pronounced photocurrent drifts are observed at all stable power levels. For future measurements, it is imperative that the device is fully insulated against moisture to eliminate this influencing factor.

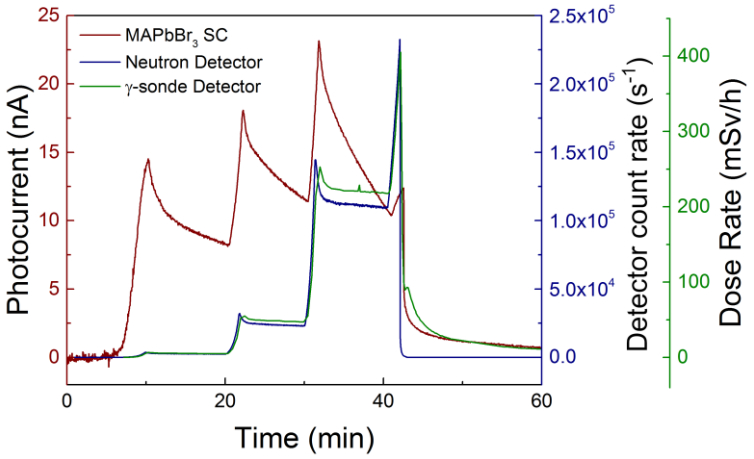

Fig. 6. Measurement of a $MAPbBr_3$ SC detector, poorly isolated against moisture, inserted in the control rod channel of the reactor core.

3 Conclusion

In conclusion, we have demonstrated that perovskite-based detectors fabricated from $MAPbBr_3$ single crystals can reliably operate within the CROCUS reactor core and its cavity. Initially, a large perovskite-based detector was tested as an ambient detector in the reactor cavity to monitor gamma dose-rate levels corresponding to varying reactor power levels. The photocurrent signal of the detector closely followed the dose-rate measurements of the gamma sonde. The detector was exposed to a gamma dose rate of 100 mSv/h for approximately 20 minutes under operational conditions without exhibiting any signs of performance degradation.

Further investigation into potential $MAPbBr_3$ SC degradation involved irradiating identical samples in the CROCUS reactor, in proximity to a gamma source, and using a Pu-Be source while maintaining the SCs at liquid nitrogen temperature. X-ray diffraction (XRD) measurements of these SC samples revealed no phase degradation. Additionally, electron paramagnetic resonance (EPR) techniques were employed to detect potential defects in the perovskite bulk material. An EPR signal was observed at several temperatures below 77 K, with a confirmed Curie-like paramagnetic temperature dependence. Upon warming the sample to room temperature, the EPR signal disappeared, suggesting the depletion of these defect states. Therefore, it can be concluded that gamma and neutron irradiation do not induce spin-bearing defects in the perovskite SC; these defects are likely trapped in existing triplet states. Results show that the perovskite material can withstand the nominal in-core operation conditions of the CROCUS reactor. Additionally, it endures tested irradiation at liquid nitrogen temperature, corresponding to a fast neutron fluence of approximately 10^{10} cm^{-2} and a gamma radiation dose of about 50 Gy, confirming only the temporary creation of defects. No signs of long-term deterioration were observed, suggesting a potential self-healing mechanism.

Finally, two perovskite-based devices, one with and one without the Gd_2O_3 neutron converter, were fabricated and tested as in-core reactor detectors. The photocurrents generated by both detectors exhibited satisfactory response times in correlation with reactor power increases. Additionally, both detectors maintained their functionality before and after irradiation in the CROCUS reactor core. However, a noticeable decrease in photocurrent was observed when the reactor power level remained stable. This decrease may be

attributed to device degradation during operation prior to the activation of the self-healing mechanism. Another plausible explanation is the high humidity levels in the control rod channel and reactor cavity during operation. Addressing this signal drift issue will be important for future studies.

References

[1] J. P. Correa-Baena *et al.*, "Promises and challenges of perovskite solar cells," *Science (80-.).*, vol. 358, no. 6364, pp. 739–744, 2017, doi: 10.1126/science.aam6323

[2] P. Andričević *et al.*, "Kilogram-Scale Crystallogenesis of Halide Perovskites for Gamma-Rays Dose Rate Measurements," *Adv. Sci.*, vol. 8, no. 2, pp. 1–9, 2021, doi: 10.1002/advs.202001882

[3] S. Yakunin *et al.*, "Detection of gamma photons using solution-grown single crystals of hybrid lead halide perovskites," *Nat. Photonics*, vol. 10, no. 9, pp. 585–589, 2016, doi: 10.1038/nphoton.2016.139

[4] K. Kim *et al.*, "Purification of CdZnTe by electromigration," *J. Appl. Phys.*, vol. 117, no. 14, pp. 1–6, 2015, doi: 10.1063/1.4917460

[5] A. Glushkova *et al.*, "Ultrasensitive 3D Aerosol-Jet-Printed Perovskite X-ray Photodetector," *ACS Nano*, vol. 15, no. 3, pp. 4077–4084, 2021, doi: 10.1021/acsnano.0c07993

[6] W. Wei *et al.*, "Monolithic integration of hybrid perovskite single crystals with heterogenous substrate for highly sensitive X-ray imaging," *Nat. Photonics*, vol. 11, no. 5, pp. 315–321, 2017, doi: 10.1038/nphoton.2017.43

[7] Y. C. Kim *et al.*, "Printable organometallic perovskite enables large-area, low-dose X-ray imaging," *Nature*, vol. 550, no. 7674, pp. 87–91, 2017, doi: 10.1038/nature24032

[8] Q. Dong *et al.*, "Electron-hole diffusion lengths > 175 um in solution-grown CH 3 NH 3 PbI 3 single crystals," *Science (80-.).*, vol. 347, no. 6225, pp. 967–970, 2015, doi: 10.1126/science.aaa5760

[9] O. Nazarenko, S. Yakunin, V. Morad, I. Cherniukh, and M. V. Kovalenko, "Single crystals of caesium formamidinium lead halide perovskites: Solution growth and gamma dosimetry," *NPG Asia Mater.*, vol. 9, no. 4, pp. e373-8, 2017, doi: 10.1038/am.2017.45

[10] C. C. Stoumpos *et al.*, "Crystal growth of the perovskite semiconductor CsPbBr3: A new material for high-energy radiation detection," *Cryst. Growth Des.*, vol. 13, no. 7, pp. 2722–2727, 2013, doi: 10.1021/cg400645t

[11] H. Wei *et al.*, "Dopant compensation in alloyed CH3NH3PbBr3−xClx perovskite single crystals for gamma-ray spectroscopy," *Nat. Mater.*, vol. 16, no. 8, pp. 826–833, 2017, doi: 10.1038/nmat4927

[12] L. Zhao *et al.*, "Surface-defect-passivation-enabled near-unity charge collection efficiency in bromide-based perovskite gamma-ray spectrum devices," *Nat. Photonics*, 2024, doi: 10.1038/s41566-023-01356-0

[13] Y. He *et al.*, "High spectral resolution of gamma-rays at room temperature by perovskite CsPbBr3 single crystals," *Nat. Commun.*, no. 2018, pp. 1–8, doi: 10.1038/s41467-018-04073-3

[14] S. I. Parkera *et al.*, "3D-A proposed new architecture for solid-state radiation detectors," *Nuclear Instruments and Methods in Physics Research A*: *Accelerators, Spectrometers, Detectors and Associated Equipment* 395.3: 328-343, 1997, doi: 10.1016/S0168-9002(97)00694-3

[15] P. Andricevic *et al.*, "Three-Dimensionally Enlarged Photoelectrodes by a

Protogenetic Inclusion of Vertically Aligned Carbon Nanotubes into CH 3 NH 3 PbBr 3 Single Crystals," 2017, doi: 10.1021/acs.jpcc.7b03421

[16] M. Spina *et al.*, "Mechanical signatures of degradation of the photovoltaic perovskite CH3NH3PbI3 upon water vapor exposure," *Appl. Phys. Lett.*, vol. 110, no. 12, 2017, doi: 10.1063/1.4978687

[17] A. Alberti, C. Bongiorno, E. Smecca, I. Deretzis, A. La Magna, and C. Spinella, "Pb clustering and PbI2 nanofragmentation during methylammonium lead iodide perovskite degradation," *Nat. Commun.*, vol. 10, no. 1, 2019, doi: 10.1038/s41467-019-09909-0

[18] F. Chen *et al.*, "Self-Assembled Growth of Ultrastable CH3NH3PbBr3 Perovskite Milliwires for Photodetectors," *ACS Appl. Mater. Interfaces*, vol. 10, no. 30, pp. 25763–25769, 2018, doi: 10.1021/acsami.8b05664

[19] S. Tóth *et al.*, "Stability and electronic properties of magnetic peapods," *Phys. Status Solidi Basic Res.*, vol. 245, no. 10, pp. 2034–2037, 2008, doi: 10.1002/pssb.200879652

[20] B. Náfrádi *et al.*, "Optically switched magnetism in photovoltaic perovskite CH 3 NH 3 (Mn:Pb)I 3," *Nat. Commun.*, vol. 7, 2016, doi: 10.1038/ncomms13406

[21] I. A. Shkrob and T. W. Marin, "Charge trapping in photovoltaically active perovskites and related halogenoplumbate compounds," *J. Phys. Chem. Lett.*, vol. 5, no. 7, pp. 1066–1071, 2014, doi: 10.1021/jz5004022

[22] F. Lang *et al.*, "Radiation Hardness and Self-Healing of Perovskite Solar Cells," *Adv. Mater.*, vol. 28, no. 39, pp. 8726–8731, 2016, doi: 10.1002/adma.201603326

[23] L. Wang *et al.*, "Development of robust perovskite single crystal radiation detectors with high spectral resolution through synergetic trap deactivation and self-healing," *InfoMat*, vol. 5, no. 9, pp. 1–12, 2023, doi: 10.1002/inf2.12461

[24] D. R. Ceratti *et al.*, "Self-Healing Inside APbBr3 Halide Perovskite Crystals," *Adv. Mater.*, vol. 30, no. 10, pp. 1–7, 2018, doi: 10.1002/adma.201706273

[25] M. Ma *et al.*, "In situ imaging of the atomic phase transition dynamics in metal halide perovskites," *Nat. Commun.*, vol. 14, no. 1, pp. 1–9, 2023, doi: 10.1038/s41467-023-42999-5

[26] C. Wang, B. R. Ecker, H. Wei, J. Huang, and Y. Gao, "Environmental Surface Stability of the MAPbBr3 Single Crystal," *J. Phys. Chem. C*, vol. 122, no. 6, pp. 3513–3522, 2018, doi: 10.1021/acs.jpcc.7b12740

[27] K. Domanski *et al.*, "Migration of cations induces reversible performance losses over day/night cycling in perovskite solar cells," *Energy Environ. Sci.*, vol. 10, no. 2, pp. 604–613, 2017, doi: 10.1039/c6ee03352k

[28] A. R. Kirmani *et al.*, "Unraveling radiation damage and healing mechanisms in halide perovskites using energy-tuned dual irradiation dosing," *Nat. Commun.*, vol. 15, no. 1, 2024, doi: 10.1038/s41467-024-44876-1

[29] M. C. De Siena *et al.*, "Extreme γ-Ray Radiation Tolerance of Spectrometer-Grade CsPbBr3 Perovskite Detectors," *Adv. Mater.*, vol. 35, no. 38, pp. 1–9, 2023, doi: 10.1002/adma.202303244

[30] Y. Miyazawa *et al.*, "Tolerance of Perovskite Solar Cell to High-Energy Particle Irradiations in Space Environment," *iScience*, vol. 2, pp. 148–155, 2018, doi: 10.1016/j.isci.2018.03.020

[31] P. Andričević *et al.*, "Hybrid halide perovskite neutron detectors," *Sci. Rep.*, vol. 11, no. 1, pp. 1–9, 2021, doi: 10.1038/s41598-021-95586-3

[32] L. Ovechkina, K. Riley, S. Miller, Z. Bell, V. Nagarkar, and K. Riley, "Gadolinium loaded plastic scintillators for high efficiency neutron detection," *Phys. Procedia*, vol. 2, no. 2, pp. 161–170, 2009, doi: 10.1016/j.phpro.2009.07.008

[33] Z. Song *et al.*, "Impact of Moisture on Photoexcited Charge Carrier Dynamics in

Methylammonium Lead Halide Perovskites," *J. Phys. Chem. Lett.*, vol. 9, no. 21, pp. 6312–6320, 2018, doi: 10.1021/acs.jpclett.8b02595